

Evaluation of the Structure of Amorphous Tungsten Oxide $W_{28}O_{72}$ by the Combination of Electron-, X-Ray- and Neutron-Diffraction (Three-Beam Experiment)

Jürgen Ankele^a, Joachim Mayer^b, Peter Lamparter^c, and Siegfried Steeb^c

^a Alcatel SEL AG, Lorenzstraße 10, D-70435 Stuttgart, Germany

^b Rheinisch-Westfälische Technische Hochschule Aachen, Gemeinschaftslabor für Elektronenmikroskopie, Ahornstraße 55, D-52074 Aachen, Germany

^c Max-Planck-Institut für Metallforschung, Heisenbergstraße 3, D-70569 Stuttgart, Germany

Reprint requests to Dr. P. L.; Fax: +49 (0)711 689-3312; E-mail: Lamparter@mf.mpg.de

Z. Naturforsch. **61a**, 189 – 196 (2006); received December 20, 2005

From the combination of quantitative electron-diffraction data with X-ray- and neutron-diffraction data (so-called three-beam experiment) the partial structure factors and pair correlation functions of amorphous sputter deposited $W_{28}O_{72}$ were determined. On the basis of the experimental atomic distances and coordination numbers, and by comparison with crystalline WO_3 , a structural model was developed, which consists of twisted WO_6 octahedra. Reverse Monte Carlo simulation in accordance with the experimental data was performed to verify the results.

Key words: Amorphous Tungsten Oxide; Diffraction; RMC Simulation.

1. Introduction

The so-called three-beam experiment, that is the combination of electron-diffraction with X-ray- and neutron-diffraction, has been considered frequently in the past as a method for contrast variation. However, in practice the combination of electrons with other radiations has been rarely applied, in contrast to that of X-rays and neutrons. This is mainly due to two reasons: (i) usually, the scattering contrast between electrons and X-rays is very small, and the selection of a suitable alloy, showing a favourable contrast, is crucial; (ii) for electron-diffraction the effects of inelastic scattering and multiple scattering are strong and thus require careful energy filtering and correction procedures.

Recently we published a method to obtain quantitative electron-diffraction data (that is the coherent elastic scattering in absolute units) for amorphous substances [1]. In the present paper we show that amorphous (a) $W_{28}O_{72}$, exhibiting sufficient contrast between electron- and X-ray-diffraction, is a suitable system for a three-beam experiment.

2. The Three-Beam Experiment

The structure of binary specimens is described by three partial structure factors $S_{ij}(Q)$ [$S_{ij}(Q) = S_{ji}(Q)$].

These determine the total structure factors $S_k(Q)$ via the so-called weighting factors $W_{k,ij}$ (in matrix notation):

$$S_k(Q) = W_{k,ij}(Q)S_{ij}(Q), \quad (1)$$

where i, j denote the atomic species 1 and 2 and k the kind of used radiation, namely electrons (E), X-rays (X), and neutrons (N), respectively. The weighting factors according to the Faber-Ziman definition [2] are given by the atomic fractions c_i and the scattering lengths $f_i(Q)$ of the constituents:

$$W_{k,ij} = c_i c_j f(Q)_{k,i} f(Q)_{k,j} / \langle f(Q) \rangle_k^2, \quad (2)$$

where $\langle f(Q) \rangle_k$ is the composition-averaged scattering length. For electrons and X-rays the terms in (1) depend on the modulus of the momentum transfer, $Q = (4\pi \sin \theta) / \lambda$, where 2θ is the scattering angle and λ the wavelength of the radiation. From three experimentally determined total $S_k(Q)$ the partial $S_{ij}(Q)$ can be calculated by inversion of the system of equations (1), provided that there is a contrast between the three experiments, i. e., the weighting factors in the three equations are different. The normalized determinant of the $W_{k,ij}$, taking values between 0 and 1, presents a measure of the contrast. While the contrast between X-rays and neutrons can be quite large, it is

generally rather small between X-rays and electrons. This is due to the fact that the ratio of the scattering lengths of two elements is not very different for X-rays (scattering from the electron shell) and electrons (scattering from the electron shell and from the nucleus). As a criterion for a successful contrast variation, using electrons and X-rays, the vector product \mathbf{C} of the corresponding two rows of the determinant of the $W_{k,ij}$ can be taken:

$$\mathbf{C} = \frac{1}{\sqrt{W_{E,ii}^2 + W_{E,ij}^2 + W_{E,jj}^2}} \begin{pmatrix} W_{E,ii} \\ W_{E,ij} \\ W_{E,jj} \end{pmatrix} \times \frac{1}{\sqrt{W_{X,ii}^2 + W_{X,ij}^2 + W_{X,jj}^2}} \begin{pmatrix} W_{X,ii} \\ W_{X,ij} \\ W_{X,jj} \end{pmatrix}. \quad (3)$$

The value of \mathbf{C} lies between 0 and 1. Consideration of the dependence of the scattering lengths on the atomic number and on the momentum transfer reveals that the combination of a light element from the upper right hand side of the periodic table with a heavy element in a binary system with higher atomic fraction of the light element favours a good contrast. Based on these criteria, a- $W_{28}O_{72}$ was chosen for the present three-beam experiment with a binary amorphous alloy. The scattering lengths for the calculation of \mathbf{C} (and for the evaluation of the experimental scattering data) were taken from [3] for neutrons, and from [4] (elastic and Compton scattering) and [5] (anomalous dispersion) for X-rays. For electrons (120 keV) the scattering lengths were calculated on the basis of values from [6], using a computer program from [7] (the values for neutral atoms were taken; see [8] for details). The values of \mathbf{C} for the tungsten oxide $W_{28}O_{72}$, plotted in Fig. 1 versus the momentum transfer Q , are in the range 0.1–0.25 and thus indeed indicate a rather good contrast in this case.

3. Experimental Procedures

3.1. Preparation of the Specimens

A reliable three-beam experiment can only be done if the specimens used for electron-, X-ray-, and neutron-diffraction are prepared in an identical way. In the present case this was the rf sputtering technique, using a Leybold-Heraeus sputtering machine of type Z 400 and a WO_3 target (Target Materials, Inc., purity 99.99%). For the electron-diffraction experiment a film with thickness of about 100 Å was sputtered on a

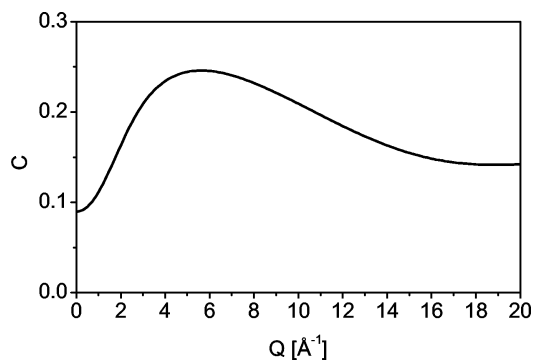


Fig. 1. Contrast \mathbf{C} according to (3) between electron- and X-ray diffraction.

freshly cleaved rock salt substrate. The substrate was removed with de-ionized water, and the amorphous film was collected on a copper grid with 10 μm mesh width, which then was used as sample holder in the electron microscope. For the X-ray-diffraction specimens with thickness of about 30 Å the substrate was a 30 μm thick Mylar[®] foil, which after fixing on a brass frame was used as sample holder. For the neutron-diffraction experiments the material was sputtered on a 50 μm thick Al foil, which afterwards was removed with a NaOH/water solution. About 8 g of the remaining amorphous tungsten oxide were filled into a vanadium cylinder as sample holder.

Chemical analysis of the sputtered tungsten oxide, using X-ray fluorescence for tungsten and carrier-gas hot extraction for oxygen, yielded the composition $W_{28}O_{72}$ with an uncertainty of about 0.5 at% and traces of a contamination with hydrogen.

The density was determined using the Archimedean method as well as X-ray reflectometry for the sputtered films and mercury porosimetry for the granular neutron sample. An average value of 8 g/cm^3 was used for the data evaluation.

3.2. Diffraction Experiments and Evaluation of Total Structure Factors

The diffraction experiments and the data correction procedures were performed in the same way as described in [1] and in detail in [8]. In particular, for the electron-diffraction experiment it was essential to suppress the inelastic scattering contribution by using the 120 keV electron microscope Zeiss EM 912 Omega, which is equipped with a so-called Omega-filter and a CCD-camera [9], and to apply a correction procedure for multiple scattering. X-ray-diffraction

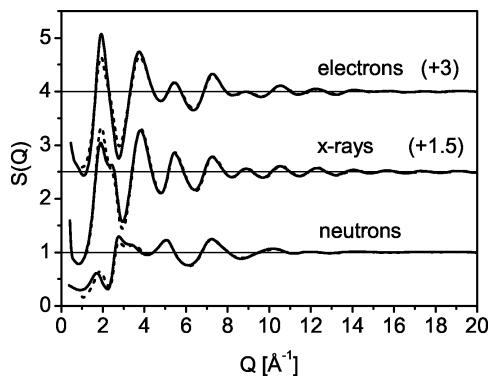


Fig. 2. Total structure factors $S(Q)$; — experimentally obtained with three different radiations; --- from RMC simulation.

was done using a laboratory-built X-ray diffractometer. The $Ag\ K\alpha$ radiation from an Ag tube was selected by using a lithium drifted silicon-detector and a multi channel analyser. Neutron-diffraction was done with the diffractometer D4 at the Institute-Laue-Langevin (ILL), Grenoble, using $\lambda = 0.4997\ \text{\AA}$. The neutron-diffraction experiment revealed that it was necessary to correct for an additional Q -dependent inelastic scattering contribution, caused by a small amount of hydrogen contained within the sample. This correction was done by Fourier-filtering (for details see [8]).

With all radiations, data up to $Q = 20\ \text{\AA}^{-1}$ could be collected.

4. Results and Discussion

4.1. Total Structure Factors

The total structure factors $S_k(Q)$ as obtained from the three diffraction experiments using electrons, X-rays and neutrons, respectively, are shown in Fig. 2 (solid lines). The X-ray curve and the neutron curve exhibit a distinct contrast due to the different weighting factors of the partial $S_{ij}(Q)$ in (1) for the two radiations (for X-rays, scattering from W is much stronger than from O , while for neutrons, scattering from O is stronger than from W). But also for electrons and X-rays a contrast occurs, mainly in the range of the first maximum. These features indicate that $a\text{-}W_{28}O_{72}$ is a suitable system for a three-beam experiment.

4.2. Partial Structure Factors and Pair Correlation Functions

From the three total structure factors the partial

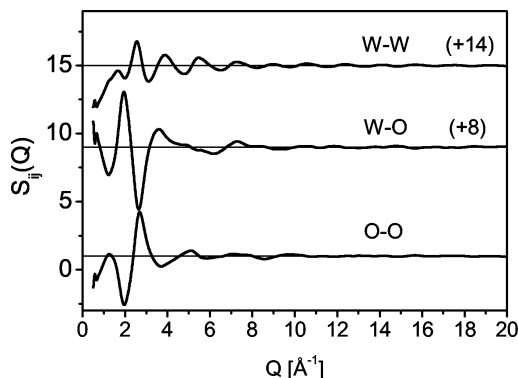


Fig. 3. Partial structure factors $S_{ij}(Q)$, experimental.

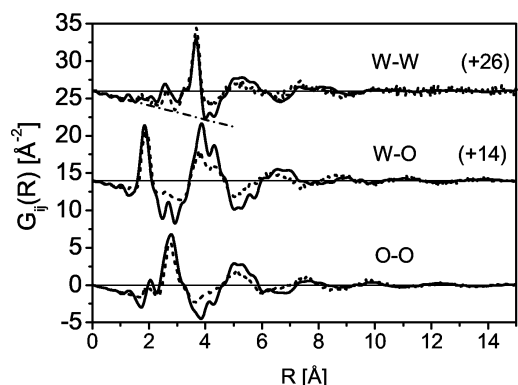


Fig. 4. Partial reduced pair distribution functions $G_{ij}(R)$; — experimental; --- from RMC simulation; —•— $-4\pi\rho_0R$ line, shown for the curve on top.

structure factors $S_{WW}(Q)$, $S_{WO}(Q)$ and $S_{OO}(Q)$ were obtained by inversion of equations (1) and are presented in Figure 3. The partial reduced pair distribution functions $G_{ij}(R)$ were calculated by Fourier transformation of the partial $S_{ij}(Q)$ according to:

$$G_{ij}(R) = 4\pi R(\rho_{ij}/c_j - \rho_0) = \frac{2}{\pi} \int_0^{\infty} (S_{ij}(Q) - 1) Q \sin(QR) dQ, \quad (4)$$

where $\rho_{ij}(R)$ is the local atomic number density of j -atoms at a distance R from an i -atom at $R = 0$, and ρ_0 is the average atomic number density. The three partial $G_{ij}(R)$ in Fig. 4 (solid lines) show pronounced maxima up to about $R = 6\ \text{\AA}$. For larger R -values the curves are only weakly oscillating, indicating a rather limited extension of the short-range order.

The atomic distances R_{ij} were taken from the positions of the peaks of $G_{ij}(R)$. For the determina-

Table 1. Atomic distances R_{ij} and partial coordination numbers Z_{ij} (j around i).

$i-j$	Peak	R_{ij} [Å]	Z_{ij}
O-W	1	1.85	1.7
	2	2.69	0.4
	3	3.87	13
W-O	1	1.85	4.4
	2	2.69	1.1
	3	3.87	33
O-O	1	2.79	14
	2	5.1	41
W-W	1	2.57	1.2
	2	3.67	4.9
	3	5.2	19

tion of the coordination numbers Z_{ij} [from the radial distribution functions $RDF_{ij}(R) = 4\pi R^2 \rho_{ij}(R) = (G_{ij}(R)/4\pi R + \rho_0)c_j$] two methods were used: Integration over the maxima between the adjacent minima and fitting (one or several) Gaussian curves to the maxima, respectively. Both methods yielded essentially the same values. (For the second peak of $G_{WO}(R)$ at $R = 2.69$ Å, which lies below the $-4\pi R\rho_0$ line, the area was limited by a straight line, connecting the adjacent minima.) The atomic distances and coordination numbers (obtained by integration) are compiled in Table 1.

4.3. Phenomenological Structure Model for a- $W_{28}O_{72}$

In the following presentation of a structural model for a- $W_{28}O_{72}$, reference is also made to the structure of crystalline (c) WO_3 [10]. In c- WO_3 each tungsten atom is at the centre of an oxygen octahedron. The WO_6 octahedra are linked via a common oxygen atom. According to the structure proposed in [11] the ranges of distances occurring in c- WO_3 are for W-O: 1.51–2.27 Å, for O-O: 2.46–2.84 Å and for W-W: 3.65–3.82 Å.

From Fig. 4 and Table 1 the following conclusions on the atomic arrangement in a- $W_{28}O_{72}$ can be obtained:

(i) $G_{WO}(R)$ shows a sharp peak at 1.85 Å with a half width of 0.34 Å.

(ii) The distance corresponding to the main maximum in $G_{WW}(R)$ at 3.67 Å is slightly smaller than the doubled W-O distance of $2 \cdot 1.85$ Å = 3.70 Å. This indicates that two W-atoms are linked together via an oxygen atom with an average W-O-W bond angle of 165°.

(iii) The coordination numbers $Z_{WO} = 4.4$ and $Z_{OW} = 1.7$ are smaller than the corresponding values 6

and 2 in c- WO_3 . This suggests that in a- $W_{28}O_{72}$, having a lower oxygen content than c- WO_3 , part of the W-atoms have no direct O-neighbours.

(iv) In c- WO_3 the coordination numbers Z_{OO} in the first ($R \approx 2.65$ Å) and second ($R \approx 3.75$ Å) coordination spheres are 8 and 6, respectively. In a- $W_{28}O_{72}$ this separation is smeared out, and we observe one main maximum at $R = 2.79$ Å, which is broadened by a satellite at 2.04 Å and a shoulder at 3.2 Å, with coordination number $Z_{OO} = 14$.

(v) Twice the first W-O distance yields 3.7 Å. At this position $G_{OO}(R)$ shows a minimum. Thus, structures with a W-atom lying just in the middle between two O-atoms can be excluded.

(vi) In c- WO_3 , W-W distances occur between 3.65 Å and 3.82 Å with coordination number $Z_{WW} = 6$. In a- $W_{28}O_{72}$ the coordination number for the main W-W peak at $R = 3.67$ Å amounts to the slightly smaller value of $Z_{WW} = 4.8$.

(vii) $G_{WW}(R)$ shows a maximum at $R = 2.57$ Å in front of the main peak with coordination number $Z_{WW} = 1.2$. This distance is smaller than the shortest W-W distance of 2.74 Å in cubic body centred W , but it agrees well with the distance of 2.6 Å occurring in molecules with covalent W-W bonds (see e.g. [12]). Thus it may be suggested that in a- $W_{28}O_{72}$, also because of the higher W-content, direct W-W pairs exist, which is not the case for c- WO_3 .

(viii) In $G_{WW}(R)$ the following relationships between distances exist:

$$1^{\text{st}} \text{ maximum: } \sqrt{2} \times 2.57 \text{ Å} = 3.63 \text{ Å} \\ \rightarrow 2^{\text{nd}} \text{ maximum,}$$

$$1^{\text{st}} \text{ maximum: } \sqrt{3} \times 2.57 \text{ Å} = 4.45 \text{ Å} \\ \rightarrow \text{shoulder on } 3^{\text{rd}} \text{ maximum,}$$

$$1^{\text{st}} \text{ maximum: } 2 \times 2.57 \text{ Å} = 5.14 \text{ Å} \\ \rightarrow 3^{\text{rd}} \text{ maximum,}$$

$$2^{\text{nd}} \text{ maximum: } \sqrt{2} \times 3.67 \text{ Å} = 5.12 \text{ Å} \\ \rightarrow 3^{\text{rd}} \text{ maximum.}$$

These relations indicate that in the structure a fraction of the W-atoms is embedded in a cubic-type arrangement. In particular, the first relation shows that two W-atoms at the distance of 3.63 Å can be linked by a third W-atom, thus forming a rectangular W-W-W triangle.

Using the properties of $G_{OO}(R)$ and $G_{WO}(R)$, a structural unit for a- $W_{28}O_{72}$ can be derived, starting from a WO_6 octahedron (Fig. 5a), which is the structural unit in c- WO_3 . By rotating the upper O-triangle by 45° (not by 60°!) the basic unit for a- $W_{28}O_{72}$ is

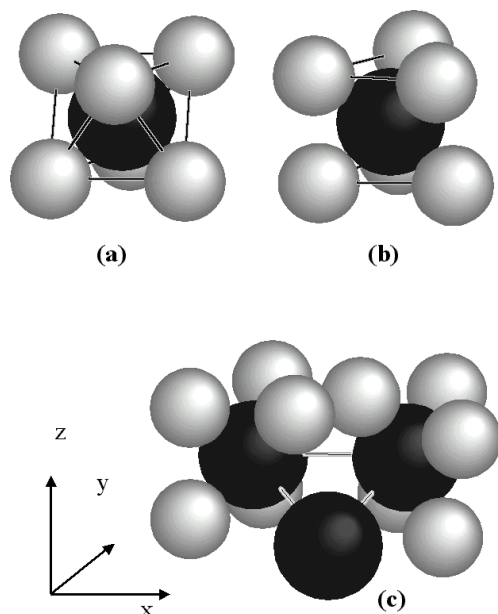


Fig. 5. Structural units: (a) octahedron of six O-atoms around a W-atom occurring in $c\text{-WO}_3$; (b) basic unit in $a\text{-WO}_3$; the upper three O-atoms are rotated by 45° ; (c) connection type *B*: two basic units are linked via a common W-atom.

obtained (Fig. 5b), which presents an intermediate arrangement between an octahedron and a trigonal prism (in fact, a distribution of rotation angles around 45° has to be assumed). This unit describes well the experimental distances and has the following properties:

(i) There are no O-atoms in direct opposition (along z -direction).

(ii) The W-O-distance amounts to 1.85 \AA .

(iii) The main peak in $G_{OO}(R)$ lies at 2.79 \AA . This distance is larger than the O-O distance $\sqrt{2} \cdot 1.85 \text{ \AA} = 2.62 \text{ \AA}$ in a regular octahedron with a W-O-distance of 1.85 \AA . Thus the structural unit of $a\text{-W}_{28}\text{O}_{72}$ must be slightly compressed in z -direction, leading to an expansion of the two O-triangles in the x, y plane (if the W-O distance is fixed), with an O-O distance of 2.79 \AA , and to a shortening of the distance in z -direction between the planes of the two O-triangles.

(iv) The shortest O-O-distance in this unit is about 2 \AA and corresponds to the satellite in $G_{OO}(R)$.

For the connection of the basic structural units, constituting the amorphous body, we propose two types:

Type *A*: Connection via a common O-atom. Here, a W-O-W connection occurs with an angle of 165° and a W-W distance of 3.67 \AA , as described above. The broad third peak of $G_{WO}(R)$ at 3.87 \AA can be assigned to the distances between a W-atom and the O-atoms

of the neighbouring basic unit. This type of connection corresponds to models of corner-sharing WO_6 octahedra as proposed in previous papers on the basis of X-ray diffraction experiments only (no partial functions) with amorphous tungsten oxides prepared by different methods: By evaporation and by reactive sputtering in [13], by electron beam evaporation at different substrate temperatures, including a post-deposition annealed sample in [14], and by thermal evaporation and by anodic oxidation in [15]. Comparison of the results, including the present ones for a sample sputtered from a tungsten oxide target, shows that the short range order, e.g., density and coordination numbers, depends on the method of production.

Type *B*: A second type of connection via a common W-atom is proposed on the basis of the partial correlation functions derived in the present work: Two basic structural units are linked via a third tungsten atom as shown in Figure 5c. The three W-atoms form an isosceles rectangular triangle, where the length of the cathetes corresponds to the first maximum of $G_{WW}(R)$ at 2.79 \AA and the length of the hypotenuse to the second maximum at 3.67 \AA . In this way, further basic units can be linked to the cluster, forming chains of W-atoms. For the connection type *B* the experimental coordination number $Z_{WO} = 4.4$ (Table 1), smaller than 6, can be explained: The two W-atoms in the centres of the basic units have 5 O-neighbours, and the connecting W-atom for spatial reasons even less neighbours (which are not shown in Fig. 5c).

The coordination number $Z_{WW} = 1.2$ (Table 1) can be interpreted as average of both types of connection, where for type *A* no direct W-neighbours and for type *B* one and two or more W-neighbours can occur.

The structural data as obtained so far by the present three-beam experiment can be explained by two types of connection of a basic structural unit (Fig. 5b). This model shall now be checked by a Monte Carlo simulation.

4.4. Reverse Monte Carlo Simulation

An amorphous $W_{28}O_{72}$ cluster was generated employing the Reverse Monte Carlo (RMC) method [16]. First, a crystalline ensemble of $11 \cdot 11 \cdot 11$ simplified octahedral WO_3 unit cells was constructed. Then randomly chosen O-atoms were removed from the ensemble until the composition $W_{28}O_{72}$ of the starting configuration was reached. During the RMC runs the closest atomic distances were set at 1.5 \AA for W-W and

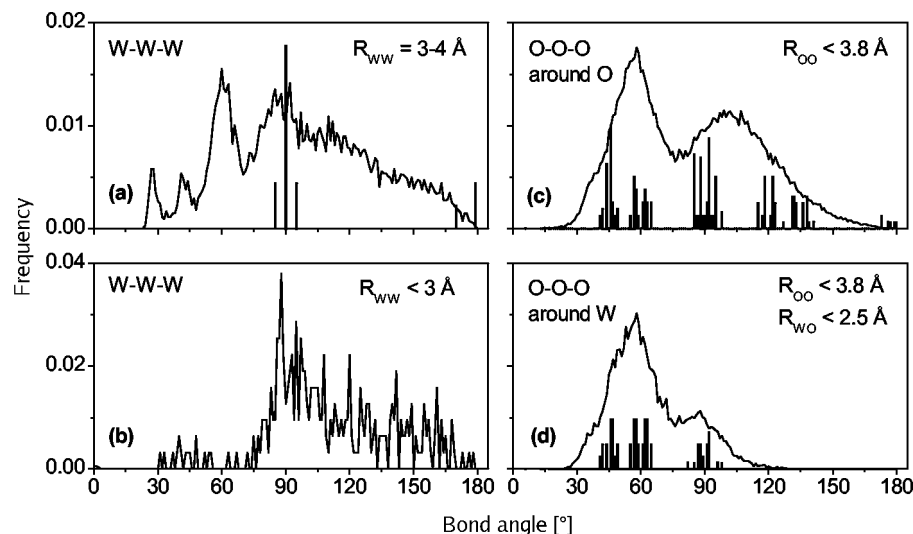


Fig. 6. Bond angle distributions from RMC simulation for W-W-W triplets (a,b), and for O-O-O triplets in coordination shell around a central O-atom (c), and in coordination shell around a central W-atom (d). The bars show the distributions for c-WO₃. The distance ranges used for the calculation are indicated.

W-O and 1.9 Å for O-O, and no constraint for coordination numbers was applied. The RMC refinement was carried out by minimization of the mean squared difference between the experimental total structure factors and those calculated from the RMC cluster.

The results are displayed in Fig. 2 (dashed lines). The overall agreement between the experimental and model curves shows that an atomic configuration is possible, which is consistent with the diffraction data obtained with the three different radiations. Only in the range of the first maximum in each case slightly different amplitudes occur (which did not improve with longer RMC runs).

Figure 4 shows the partial pair distribution functions as obtained experimentally (solid lines) and by RMC simulation (dashed lines). The RMC curves exhibit smaller amplitudes than the experimental ones with exception of the main peak of $G_{WW}(R)$.

From an analysis of the RMC cluster the histograms of coordination numbers were obtained. A comparison of the average values of the histograms with the experimental coordination numbers in Table 2 shows that the agreement between the coordination numbers obtained experimentally and by RMC simulation of a-W₂₈O₇₂ is very good and deviates only in the case of the O-O coordination.

In Fig. 6 the bond angle distributions for triples of the same type of atoms, W-W-W and O-O-O, are shown as obtained from analysis of the RMC cluster of a-W₂₈O₇₂ together with the corresponding angles in c-WO₃. The following points are of interest:

Table 2. Partial coordination numbers Z_{ij} (j around i) for the RMC cluster, from experiment and for crystalline c-WO₃. The distance-ranges used for the analysis of the RMC cluster are indicated.

$i-j$	R -range [Å]	Coordination number Z_{ij}		
		RMC	exp.	c-WO ₃
O-W	< 2.5	1.8	1.7	2
W-O	< 2.5	4.6	4.4	6
O-O	< 3.8	12	14	8
W-W	3.0–4.0	5.4	4.9	6

(i) In the W-W-W angular distribution for $R_{WW} < 3$ Å [i.e., for W-W pairs corresponding to the first maximum in $G_{WW}(R)$] only angles larger than 80° with a maximum at 90° occur (Fig. 6b). The corresponding distribution of coordination numbers for $R_{WW} < 3$ Å yields that single (41%), double (22%) and triple (5%) W-W coordination occurs (32% W-atoms have no W-neighbours). The ratio 2:1 of single and double coordination agrees with the connection type *B* as shown in Fig. 5c, where the two W-atoms in the centre of the basic units have one W-neighbour (the connecting W-atom), and the connecting W-atom has two W-neighbours.

(ii) The W-W-W angular distribution for $R_{WW} = 3-4$ Å shows pronounced maxima at 28°, 42° and 60° as well as a broad peak at 90°, which also occurs as W-W-W angle in c-WO₃ (Fig. 6a).

60°: Three W-atoms form an equilateral triangle with side length 3.67 Å.

42°: This angle occurs in an isosceles triangle with leg length 3.67 Å and base length 2.57 Å.

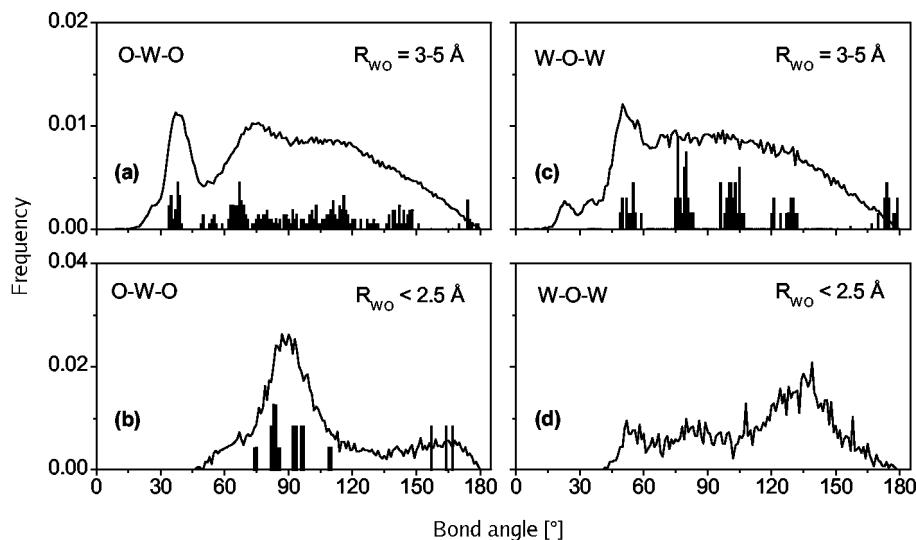


Fig. 7. Bond angle distributions from RMC simulation for O-W-O triplets (a,b), and for W-O-W triplets (c,d). The bars show the distributions for $c\text{-WO}_3$. The distance ranges used for the calculation are indicated.

(iii) The O-O-O angular distributions for $R_{OO} < 3.8 \text{ \AA}$ (Figs. 6c and d) exhibit a maximum at 60° which belongs to the equilateral O-O-O triangles of the basic structural unit (Fig. 5b). The O-O-O angular distribution of triplets belonging to a coordination shell around a central W-atom (Fig. 6d) shows a second maximum at 90° . The rotation of the upper O-O-O triangle (Fig. 5b) by rotation angles around 45° leads to a broad distribution of O-O-O angles around 90° . The O-O-O angular distribution around a central O-atom (Fig. 6c) shows a similar run as the O-O-O angular distribution around a W-atom (Fig. 6d) but with the second peak located at 115° . This difference can be explained by assuming that the involved O-atoms belong to neighbouring structural units or that they might have no direct W-neighbours.

In Fig. 7 the bond angle distributions in the triples O-W-O and W-O-W are shown. The following observations can be stated:

(i) The O-W-O and the W-O-W angular distributions for $R_{WO} = 3-5 \text{ \AA}$ [corresponding to the third maximum in $G_{WO}(R)$] extend over a large range of bond angles and show certain similarities with those for $c\text{-WO}_3$ (Figs. 7a, c).

(ii) In the O-W-O distribution a pronounced peak occurs at about 40° (Fig. 7a), which can be associated with a W-O distance of 3.87 \AA [third maximum in $G_{WO}(R)$] and an O-O distance of 2.79 \AA [first maximum in $G_{OO}(R)$].

(iii) The O-W-O distribution for $R_{WO} < 2.5 \text{ \AA}$ [corresponding to the first maximum in $G_{WO}(R)$] shows a

peak at 90° and two smaller components, around 65° and around 160° (Fig. 7b). This is in fair agreement with the basic structural unit (Fig. 5b), because for this many O-W-O angles amount to about 90° , additional angles occur around 65° and around 130° and (in contrast to a regular octahedron) no O-W-O angles occur at 180° .

(iv) The W-O-W distribution for $R_{WO} < 2.5 \text{ \AA}$ is rather broad (Fig. 7d). The peak at about 140° probably reflects the connection type A between the basic units. This angle is somewhat smaller than the angle of 165° as calculated from the W-O and W-W distances (Section 4.3).

In conclusion of this section, it can be stated that the angular distributions derived from the RMC simulation support the model cluster (Fig. 5b) proposed for the structure of amorphous $W_{28}O_{72}$.

5. Summary

As expected from the consideration of scattering contrasts, the combination of electron-, X-ray- and neutron-diffraction, the so-called three-beam experiment, can be successfully applied for the evaluation of the partial structure factors and partial pair distribution functions of amorphous $W_{28}O_{72}$. In particular, the existence of direct W-W correlations could be shown. The structure can be described with a structural model on the basis of a twisted WO_6 octahedron as a basic structural unit. The units are linked together either via a common oxygen or by a common tungsten atom. Us-

ing reverse Monte Carlo simulation, it was possible to generate an atomic configuration agreeing with the ex-

perimental structural data and the proposed structural unit.

- [1] J. Ankele, J. Mayer, P. Lamparter, and S. Steeb, *Z. Naturforsch.* **60a**, 459 (2005).
- [2] T.E. Faber and J.M. Ziman, *Philos. Mag.* **11**, 153 (1965).
- [3] V.F. Sears, *Thermal-neutron Scattering Lengths and Cross-sections for Condensed-matter Research (AECL 8490)*. Atomic Energy of Canada limited, Chalk River Nuclear Laboratories, Chalk River, ON 1984.
- [4] J. H. Hubbell, W. J. Veigele, E. A. Briggs, R. T. Brown, D. T. Cromer, and R. J. Howerton, *J. Phys. Chem. Ref. Data* **4**, 471 (1975).
- [5] Y. Waseda, *Novel Application of Anomalous (Resonance) X-Ray Scattering for Structural Characterization of Disordered Materials*, *Lecture Notes in Physics* **204**, Springer, Berlin 1984, p. 119.
- [6] P. A. Doyle and P. S. Turner, *Acta Cryst. A* **24**, 390 (1968).
- [7] A. L. Weickenmeier and H. Kohl, *Acta Cryst. A* **47**, 590 (1991) and private communication.
- [8] J. Ankele, PhD Thesis, University of Stuttgart, Stuttgart 1998.
- [9] J. Bühr, G. Benner, D. Krahl, A. Rilk, and E. Weimer, in: *Proc. 49th Ann. Meet. of the Electron Microscopy Society of America* (Ed. W. Bailey), San Francisco Press, Inc., San Francisco 1991, p. 354.
- [10] S. D. Rieck, *Tungsten and its Compounds*, Pergamon Press, Oxford 1967.
- [11] K. Schubert, *Kristallstrukturen zweikomponentiger Phasen*. Springer-Verlag, Berlin, Göttingen, Heidelberg 1964.
- [12] A. F. Holleman and E. Wiberg, *Lehrbuch der Anorganischen Chemie*, 100th ed., Walter de Gruyter, Berlin 1985.
- [13] H. R. Zeller and H. U. Beyeler, *Appl. Phys.* **13**, 231 (1977).
- [14] T. Nanba and I. Yasui, *J. Solid State Chem.* **83**, 304 (1989).
- [15] L. A. Lugovskaya, L. A. Aleshina, G. M. Kalibaeva, and A. D. Fofanov, *Acta Cryst. B* **58**, 576 (2002).
- [16] R. L. Mc Greevy and L. Pusztai, *Mol. Simulation* **1**, 359 (1988).